Point Mutations at the Type I Cu Ligands, Cys457 and Met467, and at the Putative Proton Donor, Asp105, in *Myrothecium verrucaria* Bilirubin Oxidase and Reactions with Dioxygen†

Kunishige Kataoka,‡ Rieko Kitagawa,‡ Megumi Inoue,‡ Daisaku Naruse,‡ Takeshi Sakurai,*,‡ and Hong-wei Huang§

Division of Material Sciences, Graduate School of Natural Science and Technology, Kanazawa University, Kakuma, Kanazawa 920-1192, Japan, and Accelrys KK, 3-3-1, Nishishinbashi Minato-ku, Tokyo 105-0003, Japan

Received October 30, 2004; Revised Manuscript Received March 22, 2005

ABSTRACT: The type I Cu site in the Cys457Ser mutant of *Myrothecium verrucaria* bilirubin oxidase was vacant, but the trinuclear center composed of a type II Cu and a pair of type III Cu's was fully occupied by three Cu ions. Cys457Ser could react with dioxygen, affording reaction intermediate I with absorption maxima at 340, 470, and 675 nm. This intermediate corresponds to that obtained from laccase, whose type I Cu is cupric and type II and III Cu's are cuprous [Zoppellaro, G., Sakurai, T., and Huang, H. (2001) *J. Biochem. 129*, 949−953] or whose type I Cu is substituted with Hg [Palmer, A. E., Lee, S. K., and Solomon, E. I. (2001) *J. Am. Chem. Soc. 123*, 6591−6599]. Another type I Cu mutant, Met467Gln, with modified spectroscopic properties and redox potential, afforded reaction intermediate II with absorption maxima at 355 and 450 nm. This intermediate corresponds to that obtained during the reaction of laccase [Sundaram, U. M., Zhang, H. H., Hedman, B., Hodgson, K. O., and Solomon, E. I. (1997) *J. Am. Chem. Soc. 119*, 12525−12540; Huang, H., Zoppellaro, G., and Sakurai, T. (1999) *J. Biol. Chem. 274*, 32718−32724]. According to a three-dimensional model of bilirubin oxidase, Asp105 is positioned near the trinuclear center. Asp105Glu and Asp105Ala exhibited 46 and 7.5% bilirubin oxidase activity compared to the wild-type enzyme, respectively, indicating that Asp105 conserved in all multi-copper oxidases donates a proton to reaction intermediates I and II. In addition, this amino acid might be involved in the formation of the trinuclear center and in the binding of dioxygen based on the difficulties in incorporating four Cu ions in Asp105Ala and Asp105Asn and their reactions with dioxygen.

Bilirubin oxidase (BO,[1] EC 1.3.3.5) catalyzes the oxidation of bilirubin to biliverdin, and further to a purple pigment (*1*). This reaction has been utilized in the clinical investigation of liver. BO contains one type I Cu, one type II Cu, and a pair of type III Cu's in a protein molecule (*2*−*4*), and accordingly, BO belongs to the family of multi-copper oxidases (*5*, *6*) together with laccase, ascorbate oxidase, ceruloplasmin, Fet3, CotA, CueO, and PcoA. The type I Cu mediates electron transfer from the substrate to a trinuclear center composed of the type II Cu and type III Cu's. When the trinuclear center is reduced fully, a dioxygen molecule is bound there, and is converted to two water molecules by accepting the fourth electron from the type I Cu. The type I Cu and type II Cu are EPR-detectable, but the type III Cu's are EPR-undetectable due to strong antiferromagnetic interaction through a bridged OH^-. The nucleotide sequence of the gene encoding *Myrothecium verrucaria* BO (*1*) indicated that all ligands to the four Cu ions are conserved like those of other multi-copper oxidases such as tree laccase (*7*), ascorbate oxidase (*8*), ceruloplasmin (*9*), CotA (*10*), CueO (*11*), and PcoA (*12*) (Figure 1). These multi-copper oxidases have the donor sets 1Cys2His1Met for type I Cu, 2His1H_2O (or 1OH^-) for type II Cu, and 6His1OH^- (or O^{2-}) for type III Cu's, while multi-copper oxidases such as fungal laccases (*13*−*16*) and yeast Fet3 (*17*) lack the Met for type I Cu.

The reaction of tree laccase has been studied in detail, and two reaction intermediates have been detected (*18*−*24*). One of the intermediates gave absorption maxima at 370, 420, and 670 nm (intermediate II) (*20*−*22*). According to one proposed structure, all Cu ions in the trinuclear center are cupric and are bridged by the two OH^- groups derived from dioxygen (*20*). In another proposed structure, an $O^{-\bullet}$ or $HO^{-\bullet}$ radical bridges one cuprous type II Cu with two cupric type III Cu's (*21*, *22*). These structures differ in the location of the radical center, a Cu or O atom. A stopped-flow study on the formation of this intermediate indicated that the diffusion of dioxygen to the trinuclear center is the rate-determining step and the preceding intermediate cannot be detected even if it is formed (*22*). To trap this preceding intermediate, we prepared a mixed valant laccase, in which the type I Cu was cupric and the type II Cu and type III

† This work was supported in part by a Grant-in-Aid for Scientific Research (B-13440194) from the Ministry of Education, Science, Sports and Culture of Japan (to T.S.) and by Alfresa Pharma Co.

* To whom correspondence should be addressed. Telephone: +81-76-264-5685. Fax: +81-76-264-5742. E-mail: ts0513@kenroku.kanazawa-u.ac.jp.

‡ Kanazawa University.

§ Accelrys KK.

[1] Abbreviations: BO, bilirubin oxidase; rBO, recombinant bilirubin oxidase; EPR, electron paramagnetic resonance; EDTA, ethylenediamine-*N*,*N*,*N*′,*N*′-tetraacetic acid; DPPH, 1,1-diphenyl-2-picrylhydrazyl; CD, circular dichroism; rmsd, root-mean-square deviation.

10.1021/bi0476836 CCC: $30.25
Published on Web 04/15/2005

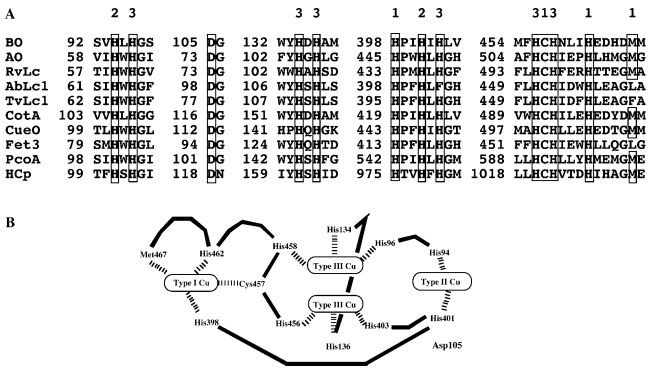

FIGURE 1: Binding sites for Cu and the putative proton donor of bilirubin oxidase in homology with those of multi-copper oxidases and their correlation. (A) Homology of partial amino acid sequence among bilirubin oxidase, ascorbate oxidase (AO), *Rhus vernicifera* laccase (RvLc), *A. thaliana* (AbLc1), *Trametes versicolor* laccase (TvLc1), CotA, CueO, Fet3, PcoA, and human ceruloplasmin (HCp). Numbers indicate the amino acids coordinating each type of Cu site. (B) Architecture of the active site showing the correlation of each Cu center and ligand amino acids.

Cu's were cuprous, by introducing a cuprous ion into a type II Cu-depleted laccase under anaerobic conditions (*23*). The reaction of this mixed valent laccase realized the trapping of intermediate I with absorption maxima at 340 and 470 nm, which should be a precursor of intermediate II. Intermediate I has been independently trapped by the reaction of laccase whose type I Cu site was substituted for Hg (*18*, *19*). Decays of intermediates I and II suggested that an amino acid with a pK_a of ~5.4 functioned as the proton donor toward dioxygen to finally produce water molecules (*18*, *21*).

Although the reaction mechanism of laccase has been extensively explored as described above, that of BO has not been studied at all. Therefore, to elucidate the reaction mechanism of BO, we designed mutants potentially suitable for trapping the reaction intermediates of BO. The Cys residue as a type I Cu ligand was substituted with Ser to exclude the masking effect of the S^- (Cys) $\rightarrow$ Cu^{2+} charge transfer (see Figure 1 for the sequence homology around the Cu-binding sites of multi-copper oxidases, including those of BO). However, the type I Cu site of the Ser mutant was vacant as in the case of the Fet3p mutant (*24*, *25*), and from the reaction of Cys457Ser, we succeeded in detecting intermediate I of BO for the first time. Further, we explored the process of reoxidation of Met467Gln because this mutant, previously prepared using *Aspergillus oryzae* as a host, exhibited peculiar enzyme activities: a drastic decrease in the activity to oxidize bilirubin and an increase in the activity to oxidize ferrocyanide by ca. 30% (*3*, *4*). We could detect intermediate II from the reaction of Met467Gln. The third mutation is of Asp105 as a putative proton donor to intermediates I and II. Asp105 was substituted with Glu, Ala, and Asn to reveal the role of this amino acid which is conserved in all multi-copper oxidases. Prior to this study, we established a new expression system for *M. verrucaria* BO using *Pichia pastoris* as a host (*26*), which enabled mass production of the recombinant BO (rBO) and mutants.

EXPERIMENTAL PROCEDURES

Site-Directed Mutagenesis of Bilirubin Oxidase. The gene fragments for mutating Cys457, Met467, and Asp105 were synthesized by PCR using the oligonucleotide primers (BEX Co. Ltd.) shown below and pBSBO harboring the complete *M. verrucaria* BO gene cloned into pBluescript II (Stratagene) as a template (sites of mutation underlined): Cys457-Ser(+), 5′-CATGTTCCATAGCCACAATTTG-3′; Cys457-Ser(−), 5′-CAAATTGTGGCTATGGAACATG-3′; Cys467-Gln(+), 5′-GGATCACGATCAGATGGCTGCC-3′; Cys467-Gln(−), 5′-GGCAGCCATCTGATCGTGATCC-3′; Asp105-Glu(+), 5′-TCTCGTGCCTTTGCCGGATGGGCA-3′; Asp-105Glu(−), 5′-TCTGCCCATCCGGCAAAGGCGG-3′; Asp-105Ala(+), 5′-TCTCGTGCCTTTGAAGGATGGGCA-3′; Asp105Ala(−), 5′-TCTGCCCATCCTTCAAAGGCGG-3′; Asp105Asn(+), 5′-TCTCGTGCCTTTAACGGATGGGCA-3′; Asp105Asn(−), 5′-TCTGCCCATCCGTTAAAGGCGG-3′.

The PCR products were digested with restriction enzymes (*Sma*I and *Not*I for Cys457Ser and Met467Gln and *Eco*RI and *Nco*I for Asp105 mutants) and exchanged with the corresponding gene fragments of pBSBO. After the verification of mutagenesis by DNA sequencing, mutated BO genes treated with *Eco*RI and *Not*I were ligated into the pPIC9K expression plasmid (Invitrogen) to give pPICBO-Cys457Ser, -Met467Gln, -Asp105Glu, -Asp105Ala, and -Asp105Asn. To enable mutant proteins to be secreted into the culture medium, the gene encoding the α-factor secretion signal of *Saccharomyces cerevisiae* was attached to the 5′-terminal end of the BO mutant genes in the pPICBO derivative (*26*).

P. pastoris GS115 was transformed by electroporation using the pPICBO derivative linearized with *Bpu*1102I. Transformants with multicopy inserts were screened for geneticin (G418) resistance. Finally, geneticin-resistant strains on YPD plates (2.0 mg/mL) were obtained for all mutants. The transformants were cultivated in 7.2 L of the BMM medium supplemented with 3×10^{-5}% $CuCl_2$ and 0.8% DL-Ala for 5 days with shaking at 25 °C with methanol added as an inducer at a final concentration of 0.5% every 24 h.

The culture medium was centrifuged at 4500 rpm for 10 min, and ammonium sulfate was added at a final concentration of 1.7 M. The medium was applied onto a Toyopearl Butyl-650 M column (ϕ, 2.5 cm × 50 cm) equilibrated with 50 mM phosphate buffer containing 1.7 M ammonium sulfate. After the unabsorbed proteins were washed away with the same buffer, the mutants were eluted with a linear gradient of ammonium sulfate (from 1.7 to 0 M). Subsequently, HiLoad Superdex 200 prep-grade 26/60 chromatography was performed using 0.1 M Tris-H_2SO_4 buffer (pH 8.5).

The purity of the final products was checked by SDS−PAGE. All mutants expressed in *P. pastoris* had a slightly higher molecular mass (66 kDa from SDS−PAGE not shown) than those expressed in *A. oryzae* (64 kDa) (*2*−*4*) because more carbohydrates were attached to them. The actions of a glycosidase, Endo H_f, in 50 mM citrate buffer (pH 5.5) at 37 °C gave the band at 60 kDa corresponding to the calculated molecular mass of 534 amino acids (data not shown).

Assaying of Enzyme Activities. The enzyme activities of the authentic BO (Amano Enzyme Inc.), rBO, and mutants for oxidizing bilirubin and ferrocyanide were determined in Tris-H_2SO_4 buffer (pH 8.4) as the decrease in absorbance at 440 nm and as the increase in absorbance at 420 nm, respectively, as reported previously (*2*−*4*).

Table 1: Absorption, CD, and EPR Spectral Data of BO and Mutants[a]

	absorption spectrum λ_{max} (nm) [ϵ (M^{-1} cm^{-1})]	CD spectrum λ_{max} (nm) [$\Delta\epsilon$ (M^{-1} cm^{-1})]	EPR spectrum $g_{II}(g_z)$, $A_{II}(A_z)$, (type)[b] ($\times 10^{-3}$ cm^{-1})
authentic BO	740 (3400), 600 (5800)	770 (−5.5), 595 (4.6), 540 (sh), 445 (−1.8), 337 (−1.0)	2.21, 8.5 (T1) 2.25, 18.6 (T2)
rBO	740 (3600), 600 (6000)	770 (−5.7), 595 (4.8), 540 (sh), 445 (−1.9), 337 (−1.0)	2.21, 8.5 (T1) 2.35, 8.4 (T3)
Cys457Ser	620 (400)	830 (0.2), 620 (−0.16), 450 (0.07), 350 (−0.17), 320 (0.24)	2.35, 8.2 (T3)
Met467Gln	860 (2500), 600 (4000)	790 (−4.4), 615 (6.2), 520 (−1.6), 450 (−5.3), 335 (−0.7)	2.28, 4.5 (T1) 2.24, 17.3 (T2)
Asp105Glu	740 (2600), 600 (4800)	770 (−3.7), 595 (5.0), 540 (sh), 440 (−1.0), 390 (0.2), 340 (−0.5)	2.21, 8.3 (T1) 2.35, 9.3 (T3)
Asp105Ala	750 (1500), 600 (2600)	755 (−2.5), 590 (3.4), 540 (sh), 445 (−1.2), 370 (0.2), 335 (−0.6)	2.22, 8.1 (T1) 2.28, 14.8 (T2)
Asp105Asn	ca. 600 (very weak)	very weak	2.35, 8.5 (T3)

[a] Measured at pH 6.0 in phosphate buffer (0.1M) at room temperature for the absorption and CD spectra and at 77 K for the EPR spectra. [b] The Cu^{2+} EPR signal with spin Hamiltonian parameters $g_{II} \sim 2.3$ and $A_{II} \sim 10 \times 10^{-3}$ cm^{-1} is denoted as T3 (type III Cu) in parentheses, although a Cu^{2+} signal not originating from T1 (type I Cu) is usually assigned to T2 (type II Cu).

Reaction of Mutants with Dioxygen. Mutants in a 0.5 cm path length quartz cell with a long neck capped with a septum were evacuated through a thin needle, and Ar was introduced. After several successive evacuations and flushings with Ar, mutants were reduced with a stoichiometric amount of dithionite. Although Met467Gln and Asp105 mutants were spontaneously reduced with the reaction of dithionite, it took ~1 h to reduce Cys457Ser. Soon after the introduction of air into the quartz cell, the absorption spectra were measured every 4 or 5 s using a spectrometer with a diode-array detector.

Instruments and Spectroscopic Measurements. Absorption spectra were measured on a JASCO Ubest 50 spectrometer and a Shimadzu MultiSpec-1500 spectrometer. CD spectra were measured on a JASCO J-500C spectropolarimeter. The X-band EPR spectra were recorded on a JEOL JES-RE1X spectrometer at 77 K and a Bruker ESP-300E spectrometer at 3−77 K. The total amount of EPR-detectable Cu^{2+} was determined by the double integration method using Cu-EDTA as a standard. Signal intensities due to the differences in tuning conditions were calibrated using 1,1-diphenyl-2-picrylhydrazyl (DPPH) as an external standard. The total amount of Cu contained in a mutant was determined by atomic absorption spectroscopy on a Varian SpectrAA-50 spectrometer. The mutations were verified by sequencing on a Hitachi SQ-5500E DNA sequencer.

Data Treatment and Modeling. Simulations of the EPR spectra and CD spectra were performed using Calleo ESR ppc and Igor Pro 5.0, respectively. A three-dimensional model of BO containing four copper ions was generated using the DS Modeler module in DS Modeling 1.1 (Accelrys Inc.). A crystal structure of CotA based on X-ray crystallography (*27*) in the Protein Data Bank (1gsk) was selected as a template whose sequence was 32% identical to that of BO. Prior to modeling, a sequence alignment between BO and 1gsk was performed using the DS Protein Family module (Align123) in DS Modeling 1.1. The three-dimensional superimposition of BO on 1gsk gave an rmsd of 0.174 nm for all aligned C-α atoms. The final three-dimensional structure of BO was visualized in DS Viewer Pro 5.0 (Accelrys Inc.).

RESULTS

Properties of Cys457Ser. Panels A and B of Figure 2 show the absorption and CD spectra of Cys457Ser at 300−800 nm, respectively (b, dotted line), together with those of rBO (a, solid line). Cys457Ser was slightly bluish at an absorption intensity ϵ of 400 at 620 nm, although rBO was intense blue with an ϵ of 6000 at 600 nm (Table 1). The band at 600 nm did not appear after reaction with ferricyanide. Therefore, it is apparent that the type I Cu was not present in Cys457Ser, consistent with the fact that Cys457Ser did not exhibit bilirubin oxidase activity (Table 2). CD spectral features of Cys457Ser were quite different from those of rBO, and intensities of all CD bands at 300−800 nm were very weak. The Cu content of Cys457Ser was 2.6 ions per protein molecule as determined by atomic absorption spectroscopy, whereas those of the authentic BO and rBO were 3.7 and 3.8 ions, respectively (Table 2). Taking into account that the experimental error in determining the Cu content of a multi-copper oxidase is ~15%, we found the type I Cu site was vacant, while the other three Cu sites were fully occupied. Therefore, Cys457Ser gave only the bands derived from the trinuclear center, the type II Cu and type III Cu's. The CD bands at 620 (−) and 830 nm (+) (the CD spectrum at 800−1000 nm is not shown) were assigned as coming from the d−d transitions. The band at 450 nm (+) was

Table 2: Bilirubin Oxidase Activity, Cu Content, and Amount of EPR-Detectable Cu^{2+} in BO and Mutants

	bilirubin oxidase activity (units/mg)[a]	average total Cu in a protein molecule[c]	average EPR-detectable Cu^{2+} in a protein molecule[d]
authentic BO	24	3.7	1.8 (T1 and T2)
rBO	24	3.8	1.9 (T1 and T3)
Cyr457Ser	~0	2.6	0.9 (T3)
Met467Gln	0.3[b]	3.9	2.0 (T1 and T2)
Asp105Glu	11	3.6	1.8 (T1 and T3)
Asp105Ala	1.2	2.7	1.4 (T1 and T2)
Asp105Asn	~0	1.6	1.4 (T3)

[a] Bilirubin oxidase activities were assayed by dissolving 2.0 mL of 30 μM bilirubin in 0.2 M Tris-H_2SO_4 buffer (pH 8.4), to which 0.2 mL of enzyme solution was added. The decrease in the absorbance at 440 nm was measured at 37 °C. One unit was defined as the amount of enzyme that oxidized 1 μmol of bilirubin/min. Activities were average values for at least three measurements. [b] Ferrocyanide oxidase activity was measured as 580 units/mg from the increase in absorption at 420 nm, while that for rBO was 430 units/mg. Other conditions were the same as for measuring the bilirubin oxidase activity. [c] Determined by atomic absorption spectroscopy. [d] The Cu^{2+} EPR signal with spin Hamiltonian parameters $g_{II} \sim 2.3$ and $A_{II} \sim 10 \times 10^{-3}$ cm^{-1} is denoted as T3 (type III Cu) in parentheses, although a Cu^{2+} signal not originating from T1 (type I Cu) is usually assigned to T2 (type II Cu).

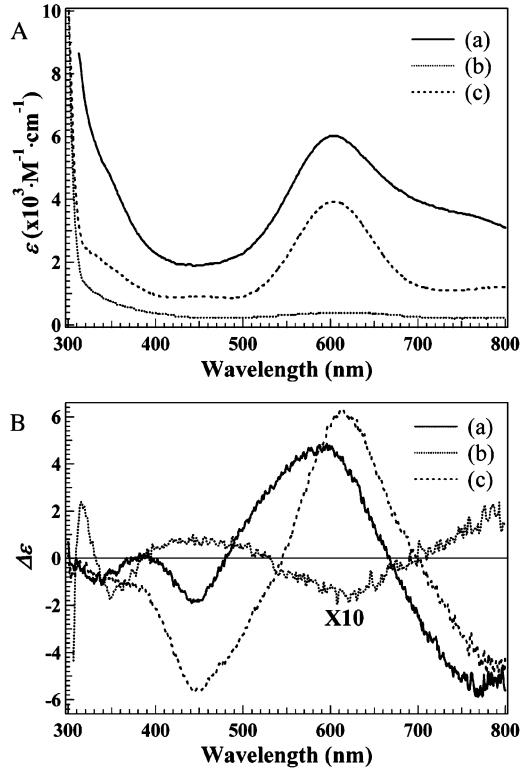

FIGURE 2: Absorption and CD spectra of the type I Cu mutants of BO. (A) Absorption spectra of rBO (a), Cys457Ser (b), and Met467Gln (c) at pH 6.0 in 0.1 M phosphate buffer. (B) CD spectra of rBO (a), Cys457Ser (b), and Met467Gln (c) at pH 6.0 in 0.1 M phosphate buffer.

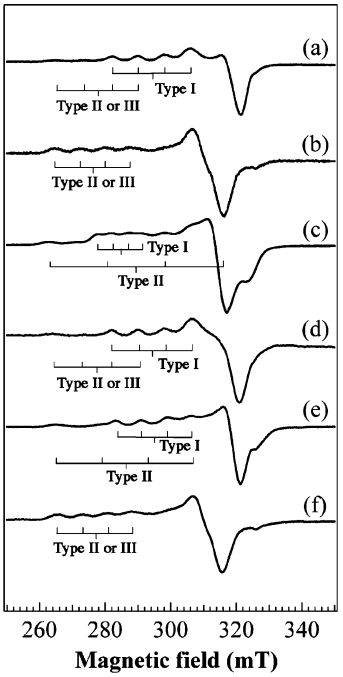

FIGURE 3: EPR spectra of rBO and mutants. X-Band EPR spectra of rBO (a), Cys457Ser (b), Met467Gln (c), Asp105Glu (d), Asp105Ala (e), and Asp105Asn (f) at 77 K. Measurement conditions: frequency, 9.20 GHz; microwave power, 4 mW; modulation, 100 kHz; modulation amplitude, 1.0 mT; filter, 0.3 s; sweep time, 4 or 8 min; amplitude, 400. The protein concentration was ca. 100 μM. The buffer solution was 0.1 M phosphate (pH 6.0).

derived from the N(His) → Cu^{2+} charge transfer, and the bands at 350 (−) and 320 (+) nm were derived from the OH^- → Cu^{2+} charge transfer. The EPR spectrum (Figure 3b) displays only the type II Cu signal with the following spin Hamiltonian parameters: $g_{II} = 2.35$, $g_\perp = 2.10$, and $A_{II} = 8.2 \times 10^{-3}$ cm^{-1} (see the Discussion for the assignment of the type of Cu). The double integration of the EPR signal showed that the total amount of EPR-detectable Cu^{2+} was 0.9 per protein molecule, indicating that approximately 2 Cu ions were present as the EPR-undetectable form, as in the case of rBO. The shoulder at ∼330 nm in the absorption spectrum (Figure 2A, b) supported the presence of the coupled type III Cu's, although its intensity was considerably weak compared to that of rBO. Therefore, a portion of the EPR-undetectable Cu might be cuprous as reported for the heterologously expressed fungal laccases (*13*−*16*).

Properties of Met467Gln. The total Cu content of Met467Gln was 3.9 ions per protein molecule as determined by atomic absorption spectroscopy, ensuring that all Cu sites were fully occupied (Table 2). The bilirubin oxidase activity exhibited by Met467Gln was only 1% of that of rBO, but the ferrocyanide oxidase activity was increased by ca. 30% compared to that of rBO (*3*) (Table 1). The absorption and CD spectra of Met467Gln are also shown in panels A and B of Figure 2, respectively (c, dashed line). Met467Gln was intense blue at an absorption intensity ϵ of 4000 at 600 nm. The d−d transition band of the authentic BO and rBO at ∼740 nm shifted to ∼860 nm for Met467Gln concomitantly with the decrease in ϵ from ∼2500 to ∼1000 (spectra at 800−1000 nm are not shown). In the CD spectrum, the sign of the band at 520 nm due to the charge transfer, S^-_σ(Cys) → Cu^{2+} (*28*), was inverted to give the negatively signed band ($\Delta\epsilon = -1.6$), and the negatively signed band at 450 nm due to the N(His) → Cu^{2+} charge transfer became considerably strong ($\Delta\epsilon = -5.3$) (Gaussian curve analysis not shown), indicating that the steric structure around the type I Cu site was significantly modified. Since the OH^- between the type III Cu's does not have the intrinsic asymmetric center, the CD band at ca. 335 nm is considerably weak, but its intensity ($\Delta\epsilon = -0.7$) is similar to that of rBO. In the EPR spectrum (Figure 3c), both type I Cu and type II Cu signals were observed with a total of 2.0 EPR-detectable Cu^{2+} atoms per protein molecule. The type I Cu signal was rhombic with the following spin Hamiltonian parameters: $g_z = 2.28$, $g_y = 2.06$, $g_x = 2.02$, $A_z = 4.5 \times 10^{-3}$ cm^{-1}, $A_y = 2.0 \times 10^{-3}$ cm^{-1}, and $A_x = 3.0 \times 10^{-3}$ cm^{-1}. The spin Hamiltonian parameters of type II Cu were as follows: $g_{II} = 2.24$, $g_\perp = 2.06$, and $A_{II} = 17.3 \times 10^{-3}$ cm^{-1}. These spectral features were the same as those of Met467Gln expressed in *A. oryzae* (*3*).

Properties of Asp105Glu, Asp105Ala, and Asp105Asn. The absorption and CD spectra of the three Asp105 mutants are shown in panels A and B of Figure 4, respectively. It is apparent that Asp105Glu (b, dotted line) fully contains type I Cu from the absorption spectrum with an ϵ of 4800 at 600 nm and from the CD spectrum in comparison with those of rBO. The presence of the coupled type III Cu's is also obvious from features at ∼330 nm in the absorption and CD spectra. The EPR spectrum exhibited two Cu signals with the following spin Hamiltonian parameters: $g_{II} = 2.21$, $g_\perp = 2.07$, and $A_{II} = 8.3 \times 10^{-3}$ cm^{-1} for type I Cu and $g_{II} = 2.35$, $g_\perp = 2.07$, and $A_{II} = 9.3 \times 10^{-3}$ cm^{-1} for type II Cu (Figure 3d). The spin Hamiltonian parameters for type I Cu were practically the same as those for the authentic BO and

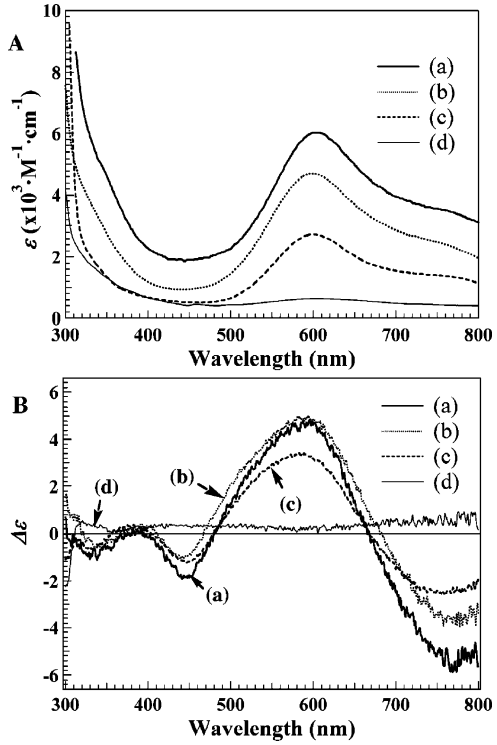

FIGURE 4: Absorption and CD spectra of the Asp105 mutants of BO. (A) Absorption spectra of rBO (a), Asp105Glu (b), Asp105Ala (c), and Asp105Asn (d) at pH 6.0 in 0.1 M phosphate buffer. (B) CD spectra of rBO (a), Asp105Glu (b), Asp105Ala (c), and Asp105Asn (d) at pH 6.0 in 0.1 M phosphate buffer.

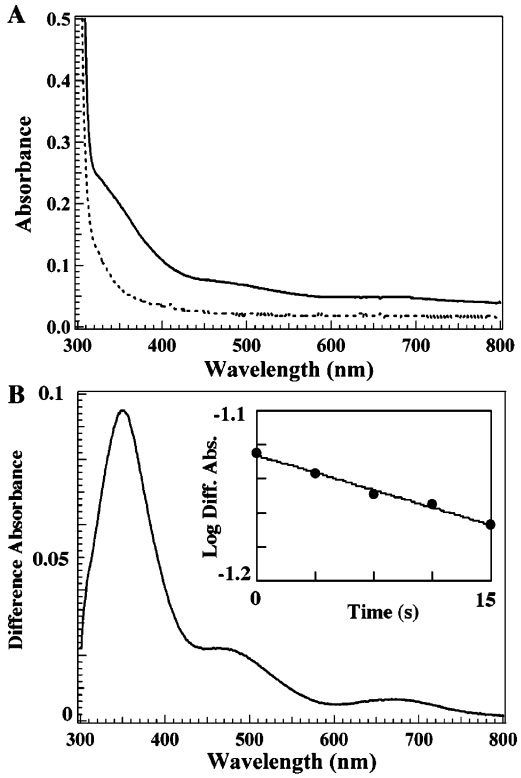

FIGURE 5: Absorption spectrum of intermediate I of Cys457Ser. Absorption spectrum of intermediate I of Cys457Ser (B) obtained by subtracting the spectrum of the reduced protein (dashed line in panel A) from that obtained soon after the reaction (solid line in panel A). The protein concentration was 225 μM. The buffer solution was 0.1 M phosphate (pH 6.0). The inset shows the decay of the absorption at 340 nm.

rBO. The spin Hamiltonian parameters for type II Cu were similar to those for rBO and Cys457Ser. The total amount of EPR-detectable Cu^{2+} was 1.8 per protein molecule. On the other hand, the total Cu content of the protein molecule was 3.6, indicating that half of the Cu ions were EPR-undetectable. The enzyme activity for oxidizing bilirubin was decreased to 46% of that of rBO by the substitution of Asp for Glu.

Asp105Ala also exhibited an intense blue color, but its absorption intensity ($\epsilon = 2600$ at 600 nm) was less than that of Asp105Glu (c, dashed line in Figure 4A). The shoulder band at 330 nm was observed, although it was not very strong. The CD spectrum afforded all the characteristics of a multi-copper oxidase, although band intensities were weaker than those for rBO (c, dashed line in Figure 4B). The EPR spectrum exhibited two Cu signals with the following spin Hamiltonian parameters: $g_{II} = 2.22$, $g_{\perp} = 2.04$, and $A_{II} = 8.1 \times 10^{-3}$ cm^{-1} for type I Cu and $g_{II} = 2.28$, $g_{\perp} = 2.04$, and $A_{II} = 14.8 \times 10^{-3}$ cm^{-1} for type II Cu (Figure 3e). Spin Hamiltonian parameters g_{II} and A_{II} for type II Cu were intermediate between those for the authentic BO and rBO. The total amount of Cu in the protein molecule was 2.7 ions as determined by atomic absorption spectroscopy. Half of all the Cu ions contained in a protein molecule (1.4 Cu) were EPR-detectable as determined by the double integration of the EPR signals, suggesting that Asp105Ala is a mixture of the mutant protein containing 4 Cu ions and apoprotein at a ratio of ~2:1 (see the Discussion). The action of Cu(I) on Asp105Ala under anaerobic conditions was unable to fully incorporate four Cu ions into the apoprotein. Further, changing the cultivation conditions was not effective in reducing the amount of apoprotein. The bilirubin oxidase activity of Asp105Ala was 5% of that of the authentic BO and rBO.

Differing from Glu and Ala mutants, Asp105Asn was colorless (d, thin line in panels A and B of Figure 4). Since oxidizing reagents such as ferricyanide did not produce an intense band at 600 nm, the type I Cu site was vacant. The EPR spectrum of Asp105Asn (Figure 3f) was similar to that of Cys457Ser (Figure 3b). The total amount of EPR-detectable Cu^{2+} was 1.4 Cu^{2+} atoms per protein molecule. Since the total Cu content of the protein molecule was determined to be 1.6 by atomic absorption spectroscopy, most of the Cu's incorporated into Asp105Asn were detected in the EPR spectrum (see the Discussion). The amount of Cu incorporated into Asp105Asn did not increase, although we changed the culture conditions.

Reaction of Cys457Ser. The reduction of Cys457Ser with a stoichiometric amount of dithionite was followed by the disappearance of the d−d band at 620 nm and the band at 315 nm (dashed line in Figure 5A). Unexpectedly, it took ~1 h to reduce Cys457Ser. However, the reduced Cys457Ser was very reactive with dioxygen, and the transient spectrum shown in Figure 5A (solid line) was obtained. Subtraction of the dashed line from the solid line gave the transient spectrum with three transient bands at 340 nm ($\epsilon = 1000$), 470 nm ($\epsilon = 200$), and 680 nm ($\epsilon = 60$) (Figure 5B). This spectrum was analogous to that observed for the reaction of the mixed valent laccase in which the type I Cu was oxidized (*23*), the reaction of laccase whose type I Cu was substituted with Hg (*18*), and the reaction of the type I Cu mutant of

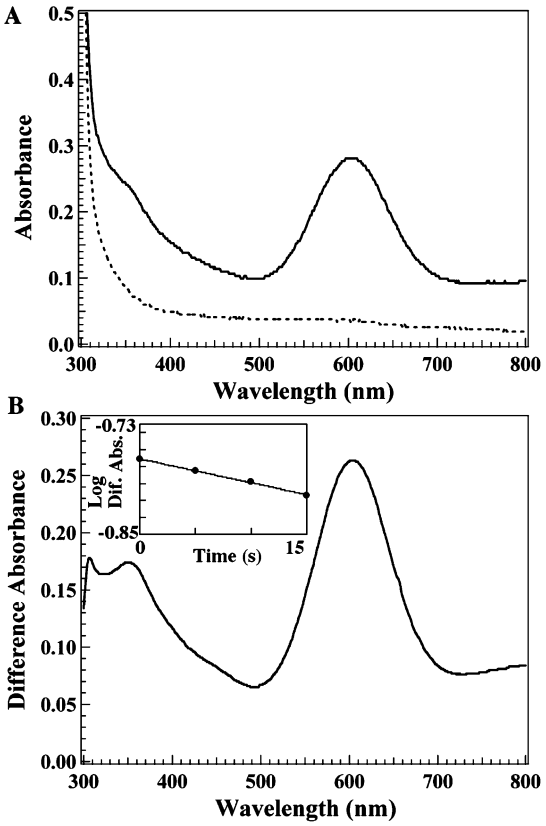

FIGURE 6: Absorption spectrum of intermediate II of Met467Gln (B) obtained by subtracting the spectrum of the reduced protein (dashed line in panel A) from that obtained soon after the reaction (solid line in panel A). The protein concentration was 124 μM. The buffer solution was 0.1 M phosphate (pH 6.0). The inset shows the decay of the absorption at 360 nm.

Fet3p, Cys484Ser (*24*, *25*). The three transient bands exponentially decayed with a k of 1.0×10^{-2} s^{-1} (inset in Figure 5B) to give an absorption spectrum similar to that of Cys457Ser. No resonance Raman band coming from this intermediate was observed (resonance Raman data not shown).

Reaction of Met467Gln. Met467Gln was reduced with a stoichiometric amount of dithionite under Ar (dashed line in Figure 6A). Unlike Cys457Ser, Met467Gln was spontaneously reduced by the action of dithionite. Soon after the reduced Met467Gln reacted with dioxygen, the blue color was restored, and the solid line in Figure 6A was obtained. Although this spectrum was analogous to that of the resting Met467Gln, the UV region was different. The difference spectrum obtained by subtracting the dashed line from the solid line (Figure 6B) showed a transient band at 360 nm, which was accompanied by a small shoulder at ~450 nm. This spectral feature was superficially similar to that observed for the reaction of Cys457Ser except for the presence of the absorption band at 600 nm, but much more similar to that observed during the reoxidation process of laccase (*21*, *22*). The transient bands exponentially decayed with a k of 1.3×10^{-2} s^{-1} (Figure 5B inset), producing a broad shoulder at 330 nm, which was present in the resting Met467Gln.

Reactions of Asp105Glu, Asp105Ala, and Asp105Asn. Asp105Glu was reduced with a stoichiometric amount of dithionite under Ar, and reacted with dioxygen. The transient spectrum (not shown), similar to that in Figure 6B, was observed for a shorter time, ~10 s. On the other hand, Asp105Ala reacted with dioxygen very slowly, and all the bands observed for it were simultaneously restored without giving a certain intermediate band. Asp105Asn did not react with dioxygen in a manner that could be detected by absorption spectroscopy.

DISCUSSION

The type I Cu site in Cys457Ser was vacant, while the trinuclear center for binding and reducing dioxygen was intact. The type I Cu mutant of Fet3p, Cys484Ser, also contained a vacant type I Cu site and gave absorption and CD spectra analogous to those of Cys457Ser BO (*24*, *25*), although many bands produced by the BO mutant shifted slightly to longer wavelengths from those of the Fet3p mutant. Only one Cu^{2+} signal was observed in the EPR spectrum of Cys457Ser BO (Figure 3b) as for Cys484Ser Fet3p. The spin Hamiltonian parameters of Cys457Ser BO ($g_{II} = 2.35$ and $A_{II} = 8.2 \times 10^{-3}$ cm^{-1}) differed considerably from those of Cys484Ser Fet3p ($g_{II} = 2.24$ and $A_{II} = 18.6 \times 10^{-3}$ cm^{-1}). A similar difference has been observed for the type II Cu in rBO expressed in *P. pastoris* or *A. oryzae* ($g_{II} = 2.35$ and $A_{II} = 8.4 \times 10^{-3}$ cm^{-1}) and that in the authentic BO ($g_{II} = 2.24$ and $A_{II} = 18.6 \times 10^{-3}$ cm^{-1}). We revealed that the authentic BO and rBO have different resting forms, but the heterologously expressed BO attains the resting form of the authentic BO after one cycle of the reaction (*29*). However, the enzyme activity of rBO was the same as that of the authentic BO (Table 2). Reinhammar reported that a type III Cu EPR signal with a g_{II} value of around 2.3 and an A_{II} value of around 10×10^{-3} cm^{-1} appears during the reaction of laccase (*30*). An EPR signal with analogous spin Hamiltonian parameters ($g_{II} = 2.33$ and $A_{II} = 10.2 \times 10^{-3}$ cm^{-1}) has been also reported for the resting CotA (*10*), being assigned to type II Cu. Any Cu^{2+} EPR signal, not originating from type I Cu, is classified as type II Cu regardless of its origin. However, to stress the difference in parameters, the EPR signals for which $g_{II} \sim 2.3$ and $A_{II} \sim 10 \times 10^{-3}$ cm^{-1} are denoted as type III Cu in parentheses in Tables 1 and 2.

Despite the difference in the amount of carbohydrates attached, the Met467Gln expressed in *P. pastoris* showed the same absorption and CD spectra as that expressed in *A. oryzae* (*3*). The red shift of the d−d transitions from that of the authentic BO by ~120 nm (Figure 2A) suggests that the type I Cu site changed from a trigonal structure with a long Cu−Met axial bond to a distorted tetrahedral structure with a shorter Cu−Gln bond (*28*, *31*). The inversion of the CD band due to type I Cu, S^{-}_{σ} (Cys) → Cu^{2+} at 520 nm, has not been reported for naturally occurring blue Cu proteins. The peculiar charge-transfer band for N(His) → Cu^{2+} at 450 nm is characteristic of blue Cu proteins such as stellacyanin and mavicyanin with the Gln coordination as the fourth ligand. The changes in structure and electronic state of type I Cu are also reflected in the EPR spectrum to give the rhombic signal (Figure 3c) characteristic of stellacyanin and mavicyanin. The drastic decrease in bilirubin oxidase activity of Met467Gln was brought about by the change in the redox potential of the type I Cu, from 470 to 270 mV (detailed electrochemical data will be published elsewhere). The electron transfer from bilirubin to the modified type I Cu site became very unfavorable since the oxidation potential of bilirubin was considerably high, ca. 500 mV (cyclic

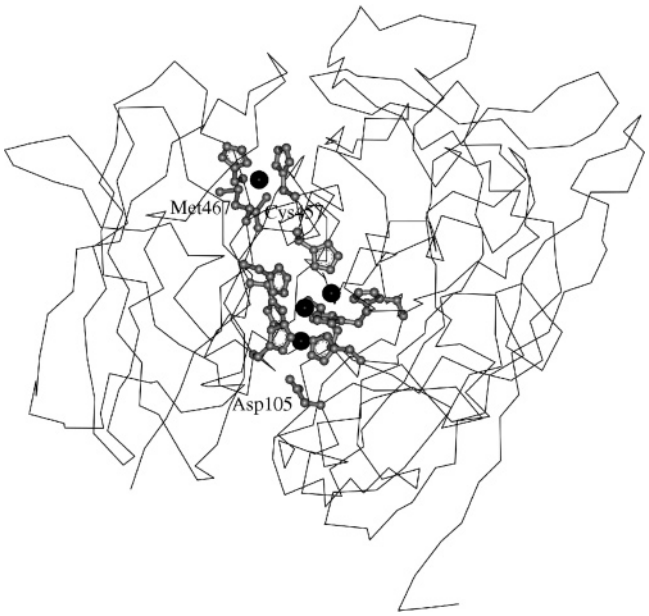

FIGURE 7: Three-dimensional view of BO derived from homology modeling. Copper atoms are represented by spheres. The side chains of the copper ligands and Asp105 are displayed. Modeling was performed with MS Modeling 3.0 (Accelrys Inc.) using data on the crystal structure of CotA (1fsk) as a template (*27*). The three-dimensional structure was produced with DS Viewer Pro 5.0.

voltammetry data not shown). However, the oxidation activity of ferrocyanide increased from 430 to 580 units/mg of protein presumably because the redox potential of the substrate, 360 mV (*32*), was not very unfavorable for reducing type I Cu compared to the case of the oxidation of bilirubin. In addition, the intramolecular electron transfer between the type I Cu and the trinuclear center became more favorable because of the change in the redox potential of type I Cu (unpublished electrochemical data).

Among the three Asp105 mutants, only Asp105Glu fully contained 4 Cu ions per protein molecule and exhibited the absorption, CD, and EPR spectra characteristic of a multi-copper oxidase (Figures 3 and 4). However, the bilirubin oxidase activity was reduced to 46% of that of the authentic BO and rBO, indicating that Asp105 conserved in all multi-copper oxidases is indeed a key amino acid in controlling the enzyme activity. According to the X-ray crystallography of multi-copper oxidases (*6*, *13*−*16*, *27*, *33*, *34*), the corresponding Asp residue is positioned at the bottom of the cavity to accommodate the trinuclear center constructed by three cupredoxin domains. Since BO has not been crystallized yet, we constructed a three-dimensional model of BO using the data from X-ray crystallography of CotA as a template (Figure 7). This model also suggests that Asp105 is positioned near the trinuclear center (vide infra) as in the case of multi-copper oxidases that have been analyzed. Therefore, Asp105 would be indispensable as a proton donor for the reaction intermediates for realizing the prompt conversion of dioxygen to water.

Even if the fact that approximately one-third of the Asp105Ala is in the apo form is taken into account, Asp105Ala containing 4 Cu ions should show 7.5% bilirubin oxidase activity compared to the authentic BO and rBO. Therefore, the bilirubin oxidase activity of Asp105Ala is still significantly weaker than that of the authentic BO and rBO, indicating that an amino acid containing a carboxylate group in its side chain is indispensable for the prompt conversion of dioxygen to water. In addition, the difficulty in fully incorporating 4 Cu ions into Asp105Ala suggests that Asp105 directly or indirectly interacts with the trinuclear center to sustain the structure of the trinuclear center. Further, at present, the possibility that Asp105 also participates in the transportation of Cu ions into the trinuclear center cannot be ruled out, although the mechanism by which Cu centers are constructed in multi-copper oxidases has not been clarified. For these reasons, approximately one-third of Asp105Ala was excreted as the apoprotein before Cu ions were incorporated.

Asp105Asn contained only 1.6 Cu^{2+} ions at the type III Cu sites as suggested by the EPR spectrum (Figure 3f). The spin Hamiltonian parameters are analogous to those of type II Cu in nitrite reductase, which originates in an unpaired type III Cu with three His coordinations from the viewpoint of molecular architecture (*35*). The type I Cu site was vacant despite the mutation at the remote amino acid residue. This presumably takes place because Asp105 is indispensable for the construction and/or maintenance of the trinuclear center, which is closely connected with the type I Cu site through the peptide backbone (Figure 1B).

The extremely slow reduction of Cys457Ser even with dithionite is evidence that the type I Cu site is positioned near the substrate-binding site and mediates the electron transfer from the substrate to the trinuclear center deeply buried inside the protein molecule. The transient spectrum (Figure 5B) derived from intermediate I gave bands at 340 ($\epsilon = 1000$), 470, and 680 nm for ~20 min. This spectrum was very similar to that obtained for the reaction of the mixed valent *Rhus vernicifera* laccacse whose type I Cu was cupric and type II and type III Cu's were cuprous (*23*) as noted in the Results. Detection of intermediate I has also been successful in the reactions of laccase whose type I Cu was substituted with Hg (*18*, *19*) and Cys484Ser Fet3p (*24*, *25*). Therefore, three multi-copper oxidases, BO, laccase, and Fet3p, afford the common intermediate I, when the one-electron-deficient derivatives are formed. No new signal was observed in the EPR spectra at 4−77 K, indicating that intermediate I was EPR-undetectable as in the case of laccase and Fet3p (*18*, *19*, *23*−*25*). In the study on laccase (*23*), we proposed a peroxide-bound structure for intermediate I (Figure 8). Solomon et al. (*18*, *19*) referred to intermediate I as a peroxide-level intermediate, proposing a similar structure. However, the five-centered complexes, 2Cu(II)-1Cu(III)2O^{2-} , in which three Cu ions are bridged by two O^{2-} groups, gave analogous absorption spectra with three bands at 342, 515, and 685 nm (*36*, *37*). These models indicated that it becomes possible to simultaneously transfer four electrons to a dioxygen molecule by using a Cu(III) state. The Cu(III) ion returns to the Cu(II) state when it receives an electron from type I Cu. At present, it is difficult to determine which model is more appropriate for the structure of intermediate I.

The bilirubin oxidase activity of Met467Gln was significantly low, only 0.4% of that of rBO. A shift in the redox potential of the type I Cu by 200 mV in the negative direction made the electron transfer from bilirubin to type I Cu extremely unfavorable, leading to the drastic decrease in activity. However, the reaction of the reduced Met467Gln

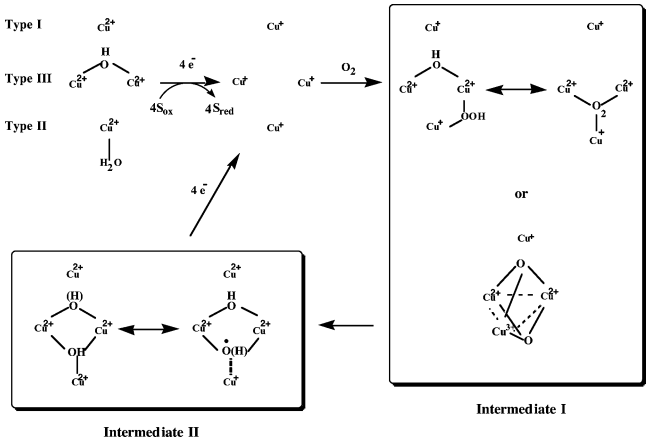

FIGURE 8: Reaction of BO to reduce dioxygen to water. Intermediate I, detected in the reaction of Cys457Ser, has a peroxide structure or five-centered structure with a 2Cu(II)1Cu(III) core. Intermediate II, detected in the reaction of Met467Gln, has a doubly hydroxide-bridged structure or oxygen-centered radical structure.

with dioxygen gave intermediate II with an absorption maximum at 360 nm (Figure 6B), similar to that obtained during the reaction of the reduced laccase with dioxygen (*20*−*23*). An analogous transient spectrum could be observed in the reaction of the authentic BO (not shown), although it was not as clear as in Figure 6B.

Since both intermediates I and II are commonly observable for BO, laccase, and Fet3p, the reduction of a dioxygen molecule proceeds via intermediate I followed by the formation of intermediate II, finally leading to the production of two molecules of water. The total reaction scheme is shown in Figure 8. If intermediate I has a five-centered structure as shown in Figure 8, its conversion to intermediate II may proceed very smoothly with the transfer of the final electron from the type I Cu to the Cu(III) ion, followed by deformation to break some Cu−O bonds. Simultaneously, the transfer of a proton from Asp105 to O^{2-} may take place. On the other hand, if intermediate I is in the peroxide form, many steps are required to reach intermediate II. The conversion of dioxygen to water by a multi-copper oxidase differs considerably from that by a cytochrome oxidase, which passes through a number of processes as has been revealed by the time-resolved resonance Raman investigation (*38*).

When Asp105 was substituted with Glu, the mutant contained four Cu ions, but its bilirubin oxidase activity was 46% of that of the authentic BO and of rBO. The decrease in bilirubin oxidase activity would have been brought about by a change in the spatial arrangement of the carboxyl group. According to the model structure of BO (Figure 7), Asp105 is positioned near the trinuclear center as in the case of ascorbate oxidase (*6*), CotA (*27*), CueO (*33*), and fungal laccases (*13*−*16*). The distance between an oxygen atom in the side chain of Asp105 and type II Cu is ∼0.8 nm, enabling interaction through a hydrogen bond via water molecules. Further, the distance between an oxygen atom in the side chain of Asp and the HN group in the imidazole ring of His403, a ligand to one of the type III Cu's, is <0.3 nm, allowing direct interaction through a hydrogen bond. In the reduced form of ascorbate oxidase, the triangle formed by the three Cus becomes larger to accommodate a dioxygen molecule (*6*), although there is no definite information about the structural change during the reduction of dioxygen. Consistent with this, we showed that considerable structural change takes place during the decay of intermediate II of laccase with an enthalpy and entropy of activation of 37−58 kJ/mol and −143 to −58 J K^{-1} mol^{-1}, respectively, highly dependent on the pH (*21*).

The slow and/or incomplete incorporation of Cu ions into Asp105Ala and Asp105Asn suggests that the Asp residue conserved in all multi-copper oxidases is indispensable to the formation of the trinuclear center, although the mechanism by which Cu ions are incorporated into an apo multi-copper oxidase after translation has not been elucidated. In some metalloproteins, amino acids that deliver a specific metal ion to the active site have been discovered (*39*). Further, even if the presence of an apoprotein was taken into account, the bilirubin oxidase activity of Asp105Ala containing 4 Cu ions was only ∼7.5% of that of the authentic BO or rBO. The reoxidation of Asp105Ala proceeded very slowly, restoring the bands at 600 and 330 nm simultaneously. These results strongly suggest that the affinity for dioxygen was significantly decreased by the point mutation replacing Asp105 with Ala. Although we have not determined the binding constant of dioxygen, Asp105 might be involved in the binding of dioxygen at the trinuclear center. Novel information obtained from Asp105 mutants is that this amino acid may play a key role not only in the supply of H^+ to dioxygen but also in the formation of the trinuclear center and binding of dioxygen.

CONCLUSIONS

Cys457Ser, a mutant for the type I Cu site, gave a vacant type I Cu site but could react with dioxygen, allowing the detection of intermediate I, which could not be detected in the reaction pathway of the authentic BO and rBO. Met467Gln, another mutant for the type I Cu site, enabled detection of intermediate II, which is an oxidized form attained just before the resting form. Mutations at a noncoordinating amino acid, Asp105, suggested that it not only donates a proton to dioxygen but also is involved in the formation of the trinuclear center and in the binding of dioxygen.

REFERENCES

1. Koikeda, S., Ando, K., Kaji, H., Inoue, T., Murao, S., Takeuchi, K., and Samejima, T. (1993) Molecular cloning of the gene for bilirubin oxidase from *Myrothecium verrucaria* and its expression in yeast, *J. Biol. Chem. 268*, 18801−18809.
2. Shimizu, A., Kwon, J.-H., Sasaki, T., Satoh, T., Sakurai, N., Sakurai, T., Yamaguchi, S., and Samejima, T. (1999) *Myrothecium verrucaria* bilirubin oxidase and its mutants for potential copper ligands, *Biochemistry 38*, 3034−3042.
3. Shimizu, A., Sasaki, T., Kwon, J.-H., Okara, A., Satoh, T., Sakurai, N., Sakurai, T., Yamaguchi, S., and Samejima, S. (1999) Site-directed mutagenesis of a possible type I copper ligand of bilirubin oxidase: A Met467Gln mutant shows stellacyanin-like properties, *J. Biochem. 125*, 662−668.
4. Shimizu, A., Samejima, T., Hirota, S., Yamaguchi, S., Sakurai, N., and Sakurai, T. (2003) Type III mutants of *Myrothecium verrucaria* bilirubin oxidase, *J. Biochem. 133*, 767−772.
5. Solomon, E. I., Sundaram, U. M., and Machonkin, T. E. (1996) Multicopper oxidases and oxygenases, *Chem. Rev. 96*, 2563−2605.
6. Messerschmidt, A., Ladenstein, R., Huber, R., Bolognesi, M., Avigliano, L., Petruzzelli, R., Rossi, A., and Finazzi-Agro, A. (1992) Refined crystal structure of ascorbate oxidase at 1.9 Å resolution, *J. Mol. Biol. 224*, 179−205.

7. Nitta, K., Kataoka, K., and Sakurai, T. (2002) Primary structure of a Japanese lacquer tree laccase as a prototype enzyme of multicopper oxidases, *J. Inorg. Biochem. 91*, 125−131.
8. Okawa, J., Okada, A., Shinmyo, M., and Takano, M. (1989) Primary structure of cucumber (*Cucumis sativus*) ascorbate oxidase deduced from cDNA sequence: Homology with blue copper proteins and tissue specific expression, *Proc. Natl. Acad. Sci. U.S.A. 86*, 1239−1243.
9. Takahashi, N., Bauman, R. A., Ortel, T. L., Dwulet, F. E., Wang, C., and Putnam, F. W. (1883) Internal triplication in the structure of human ceruloplasmin, *Proc. Natl. Acad. Sci. U.S.A. 80*, 115−119.
10. Martins, L. O., Soares, C. M., Pereira, M. M., Teixeira, M., Costa, T., Jones, G. H., and Henriques, A. O. (2002) Molecular and biochemical characterization of a highly stable bacterial laccase that occurs as a structural component of the *Bacillus subtilis* endospore coat, *J. Biol. Chem. 277*, 18849−18859.
11. Welch, R. A., Burland, G., Plunkett, G., III, Redford, P., Roesch, P., Rasko, D., Buckles, E. L., Liou, S. R., Boutin, A., Hackett, J., Stroud, D., Mayhew, G. F., Rose, D. J., Zhou, S., Schwartz, D. C., Perna, N. T., Mobley, H. L. T., Donnenberg, M. S., and Blattner, F. R. (2002) Extensive mosaic structure revealed by the complete genome sequence of uropathogenic *Escherichia coli*, *Proc. Natl. Acad. Sci. U.S.A. 99*, 17020−17024.
12. Brown, N. L., Barrett, S. R., Camakaris, J., Lee, B. T., and Rouch, D. A. (1995) Molecular genetics and transport analysis of the copper-resistance determinant (pco) from *Escherichia coli* plasmid pRJ1004, *Mol. Microbiol. 17*, 1153−1166.
13. Ducros, V., Brzozowski, A. M., Wilson, K., Brown, S. H., Ostergaard, P., Schneider, P., Yaver, D. S., Pedersen, A. H., and Davies, G. J. (1998) Crystal structure of the type-2 Cu depleted laccase from *Coprinus cinereus* at 2.2 Å resolution, *Nat. Struct. Biol. 5*, 310−316.
14. Piontek, K., Antorini, M., and Choinowski, T. (2002) Crystal structure of a laccase from the fungus *Trametes versicolor* at 1.9 Å resolution containing a full complement of coppers, *J. Biol. Chem. 40*, 37663−37669.
15. Bertrand, T., Jolivalt, C., Briozzo, P., Caminade, E., Joly, N., Madzak, C., and Mougin, C. (2002) Crystal structure of a four-copper laccase complexes with an arylamine: Insights into substrate recognition and correlation with kinetics, *Biochemistry 41*, 7325−7333.
16. Hakulinen, N., Kiiskinen, L.-L., Kruus, K., Saloheimo, M., Paananen, A., Koivula, A., and Rouvinen, J. (2002) Crystal structure of a laccase from *Melanocarpus albomyces* with an intact trinuclear copper site, *Nat. Struct. Biol. 9*, 601−605.
17. Askwith, C., van Ho, A., Bernard, P. S., Davis-Kaplan, S., Sipe, D. M., and Kaplan, J. (1994) The FET3 gene of *S. cerevisiae* encodes a multicopper oxidase required for ferrous iron uptake, *Cell 28*, 403−410.
18. Shin, W., Sundaram, U. M., Cole, J. L., Zhang, H. H., Hedman, B., Hodgson, K. O., and Solomon, E. I. (1996) Chemical and spectroscopic definition of the peroxide-level intermediate in the multicopper oxidases: Relevance to the catalytic mechanism of dioxygen reduction to water, *J. Am. Chem. Soc. 118*, 3202−3215.
19. Palmer, A. E., Lee, S. K., and Solomon, E. I. (2001) Decay of the peroxide intermediate in laccase: Reductive cleavage of the O−O bond, *J. Am. Chem. Soc. 123*, 6591−6599.
20. Lee, S.-K., George, S. D., Antholine, W. E., Hedman, B., Hodgson, K. O., and Solomon, E. I. (2002) Nature of the intermediate formed in the reaction of O_2 to H_2O at the trinuclear copper cluster active site in native laccase, *J. Am. Chem. Soc. 124*, 6180−6193.
21. Huang, H.-W., Zoppellaro, G., and Sakurai, T. (1999) Spectroscopic and kinetic studies on the oxygen-centered radical formed during the four-electron reduction process of dioxygen by *Rhus vernicifera* laccase, *J. Biol. Chem. 274*, 32718−32724.
22. Zoppellaro, G., Huang, H.-W., and Sakurai, T. (2000) Kinetic studies on the reaction of the fully reduced laccase with dioxygen, *Inorg. React. Mech. 2*, 79−84.
23. Zoppellaro, G., Sakurai, T., and Hang, H.-W. (2001) A novel mixed valence form of *Rhus vernicifera* laccase and its reaction with dioxygen to give a peroxide intermediate bound to the trinuclear center, *J. Biochem. 129*, 949−953.
24. Blackburn, N. J., Ralle, M., Hassett, R., and Kosman, D. J. (2000) Spectroscopic analysis of the trinuclear cluster in the Fet3 protein from yeast, a multicopper oxidase, *Biochemistry 39*, 2316−2324.
25. Palmar, A. E., Quintanar, L., Severance, S., Wang, T., Kosman, D. J., and Solomon, E. I. (2002) Spectroscopic characterization and O_2 reactivity of the trinuclear Cu cluster of mutants of the multicopper oxidase Fet3p, *Biochemistry 41*, 6438−6448.
26. Kataoka, K., Tanaka, K., and Sakurai, T. (2003) JP Patent 310979. Kataoka, K., Tanaka, K., Sakai, Y., and Sakurai, T. (2005) High-level expression of *Myrothecium verrucaria* bilirubin oxidase in *Pichia pastoris*, and its facile purification and characterization, *Protein Expression Purif. 41*, 77−83.
27. Enguita, F. J., Martins, L. O., Henriques, A. O., and Carrondom, M. A. (2003) Crystal structure of a bacterial endospore coat component: A laccase with enhanced thermostability properties, *J. Biol. Chem. 278*, 19416−19425.
28. Solomon, E. I., Szilagyi, R. K., Geroge, S. D., and Basumallick, L. (2004) Electronic structures of metal sites in proteins and models: Contribution to function in blue copper proteins, *Chem. Rev. 104*, 419−458.
29. Sakurai, T., Zhang, L., Fujita, T., Kataoka, K., Shimizu, A., Samejima, T., and Yamaguchi, S. (2003) Authentic and recombinant bilirubin oxidases are in different resting forms, *Biosci., Biotechnol., Biochem. 67*, 1157−1159.
30. Reinhammar, B. (1984) in *Copper Proteins and Copper Enzymes* (Lontie, R., Ed.) Vol. 3, pp 1−35, CRC Press, Boca Raton, FL.
31. Harrison, M. D., and Dennison, C. (2004) An axial Met ligand at a type I copper site is preferable for fast electron transfer, *ChemBioChem 5*, 1579−1581.
32. Day, R. A., Jr., and Underwood, A. L. (1967) *Quantitative Analysis*, 2nd ed., Prentice-Hall, Englewood Cliffs, NJ.
33. Roberts, S. A., Weichsei, A., Grass, G., Thakali, K., Tollin, G., Rensing, C., and Montfort, W. (2002) Crystal structure and electron-transfer kinetics of CueO, a multicopper oxidase required for copper homeostasis in *Escherichia coli*, *Proc. Natl. Acad. Sci. U.S.A. 99*, 2766−2771.
34. Zaitseva, I., Zaitsev, V., Card, G., Moshkov, K., Bax, B., Ralph, A., and Lindley, P. (1996) The X-ray structure of human serum ceruloplasmin at 3.1 Å: Nature of the copper centres, *J. Biol. Inorg. Chem. 1*, 15−23.
35. Adman, E. T., Godden, J. E., and Turley, S. (1995) The structure of copper-nitrite reductase from *Achromobacter cycloclastes* at five pH values, with NO_2 bound and with type II copper depleted, *J. Biol. Chem. 270*, 27458−27474.
36. Cole, A. P., Root, D. E., Mukherjee, P., Solomon, E. I., and Stack, T. D. P. (1996) A trinuclear intermediate in the copper-mediated reduction of O_2: Four electrons from three coppers, *Science 273*, 1848−1850.
37. Taki, M., Teramae, S., Nagatomo, S., Tachi, Y., Kitagawa, T., Itoh, S., and Fukuzumi, S. (2002) Fine-tuning of copper(I)-dioxygen reactivity by 2-(2-pyridyl)ethylamine bidentate ligands, *J. Am. Chem. Soc. 124*, 6367−6377.
38. Kitagawa, R., and Ogura, T. (1998) Time-resolved resonance Raman investigation of oxygen reduction mechanism of bovine cytochrome *c* oxidase, *J. Bioenerg. Biomembr. 30*, 71−79.
39. Kuchar, J., and Hausinger, R. P. (2004) Biosynthesis of metal sites, *Chem. Rev. 104*, 509−525.

BI0476836